JDI Journal of Diabetes Investigation Open access
Official Journal of the Asian Association for the Study of Diabetes
ORIGINAL ARTICLE

Immunoglobulin heavy constant gamma 1 silencing decreases tonicity-responsive enhancer-binding protein expression to alleviate diabetic nephropathy

Qibo Hu[1], Qingxiao Yang[2], Hang Gao[3], Jing Tian[1], Guanghua Che[1]*

[1]Department of Pediatrics, The Second Hospital of JiLin University, Changchun, China, [2]Department of Neurosurgery, The Second Hospital of JiLin University, Changchun, China, and [3]The Key Laboratory of Pathobiology, Ministry of Education, Norman Bethune College of Medicine, JiLin University, Changchun, China

Keywords
Bioinformatics analysis, Diabetic nephropathy, IGHG1

***Correspondence**
Guanghua Che
Tel.: +86-0431-81136555
Fax: +86-0431-81136555
E-mail address:
chegh@jlu.edu.cn

J Diabetes Investig 2024; 15: 572–583

doi: 10.1111/jdi.14144

ABSTRACT

Aims/Introduction: The molecular mechanisms of diabetic nephropathy (DN) are poorly identified. However, the advantage of an increasing amount on microarray data of diabetic nephropathy intrigued us to explore the mechanisms based on bioinformatics prediction for diabetic nephropathy.

Materials and Methods: Bioinformatics analysis was conducted to screen the hub genes associated with diabetic nephropathy. The average human renal tubular epithelial cells were exposed to high glucose (HG) to generate an *in vitro* cell model. In addition, a mouse model of diabetic nephropathy was established using a high-fat diet and streptozotocin injection. Finally, the shRNA targeting immunoglobulin heavy constant gamma 1 (IGHG1) was introduced *in vitro* and *in vivo* to illustrate its effect on downstream factors and on the development diabetic nephropathy.

Results: Bioinformatics analysis revealed that IGHG1, TRIM11 (tripartite motif protein 11), and TonEBP are highly expressed in diabetic nephropathy. *In vitro* cell experiments demonstrated that IGHG1 positively regulates the expression of TRIM11 and TonEBP (tonicity-responsive enhancer binding protein) in HK2 cells treated with high glucose. Furthermore, TRIM11 upregulates the expression of TonEBP through activation of the MEK/ERK (mitogen-activated protein kinase/extracellular signal-regulated kinase) signaling pathway in HK2 cells treated with high glucose. *In vivo*, animal experiments further confirmed that silencing IGHG1 could prevent the occurrence and development of diabetic nephropathy.

Conclusion: The silencing of IGHG1 alleviated diabetic nephropathy by inhibiting the TRIM11/MEK/ERK axis and by downregulating TonEBP.

INTRODUCTION

Diabetic nephropathy (DN), as a complication of diabetes mellitus (DM) inducing the progression of end-stage renal disease[1,2], is a notable contributor to the alarming mortality for patients with diabetes mellitus[3,4]. Diabetic nephropathy can be diagnosed through pathologic structural and functional alterations in the kidneys of patients with diabetes mellitus, characterized by hypertension, progressive kidney function decline, and proteinuria[5]. The complex organ pathology in patients with diabetes mellitus, with a series of profound structural, metabolic, and functional alterations, challenges the development of efficient therapies for diabetic nephropathy[6]. Consequently, it is of growing interest to delve into the pathogenic mechanisms underlining diabetic nephropathy for developing novel strategies for diabetic nephropathy.

Immunoglobulin G (IgG) is an essential component of human adaptive immunity, accounting for approximately 80%

Received 16 June 2023; revised 14 December 2023; accepted 21 December 2023

of total immunoglobulins[7]. It has been shown that the glomerular IgG deposit impacts the glomerular structure and emerges as an independent risk factor for diabetic nephropathy[8]. Also, prior evidence has suggested that urinary IgG was elevated as diabetic nephropathy progressed[9]. Immunoglobulin heavy constant gamma 1 (IGHG1), as a member of the IgG subclass, is a critical functional isoform of immunoglobulins produced by the immune system of the body[10–12]. IGHG1 is among the urinary glycoproteins related to chronic kidney disease[13], having a predictive potential for response to steroid therapy in focal segmental glomerulosclerosis[14]. An earlier study elucidated that IGHG1 was correlated with kidney injuries in chronic kidney disease[15]. Thus, the research on IGHG1 is vital for understanding the pathological mechanisms underlying diabetic nephropathy.

As a type I interferon-inducible E3 ligase, the tripartite motif-containing (TRIM) protein family orchestrates multiple cell functions, such as transcription, signal transduction, and cell cycle progression[16]. Of note, TRIM11 has been classified as participating in the development of diabetic nephropathy[17]. Intriguingly, research by Di *et al.*[18] uncovered that TRIM11-knocked down glioma cells exhibited a decline in the activity of the MEK/ERK pathway. More importantly, the activation of the MEK/ERK pathway has been implicated in progression of diabetic nephropathy[19]. A prior study demonstrated the activating impacts of the MEK/ERK pathway on tonicity-responsive enhancer-binding protein (TonEBP) after NRK52E cells were treated with NaCl or mannitol hyperosmolality[20]. Furthermore, TonEBP expression is high in adrenocortical tubular cells of diabetic transgenic mice, accompanied by vacuolated degenerative changes[21]. Accordingly, the TRIM11/MEK/ERK/TonEBP axis might be involved in the onset and development of diabetic nephropathy.

Nevertheless, limited data focused on the relationship between IGHG1 and TRIM11 and their functional relevance in diabetic nephropathy. Therefore, this study sought to ascertain whether IGHG1 orchestrates the progression of diabetic nephropathy *via* the TRIM11/MEK/ERK/TonEBP axis.

MATERIALS AND METHODS

Retrieval of differentially expressed genes (DEGs)

The GEO database was utilized to retrieve the dataset GSE86300, which is relevant to diabetic nephropathy. This dataset consists of five samples of early-stage diabetic mouse renal cortex tissues and five control samples of mouse renal cortex tissues. Differential mRNA analysis was performed using the criteria of $|\log FC| > 2.25$ and a P value < 0.05, with the aid of the "limma" package in R language to identify genes with differential expression. In addition, two validation datasets, GSE20636 (including six samples of late-stage diabetic mouse kidney tissues (8 months old) and six control samples of mouse kidney tissues) and GSE185616 (comprising five samples of late-stage diabetic mouse renal cortex tissues and 12 control samples of mouse renal cortex tissues), were included.

Cell culture and short hairpin RNA transduction

Human renal tubular epithelial cells HK-2 (CRL-2190) were cultured in DMEM/F12 (Gibco, USA) medium supplemented with streptomycin (100 U/mL; Gibco, MA, USA), penicillin (100 U/mL; Gibco), and 10% FBS (Gibco). The cells were maintained in a CO_2 incubator at 37°C. For the control group, the cells were treated with 5.5 mM glucose for 24 h, while the high glucose group (HG) cells were treated with 30 mM glucose for 24 h.

The isolation and induction of bone marrow-derived macrophages (BMDM) was performed as follows. Six-week-old mice were euthanized, and the femurs and tibias were flushed with phosphate-buffered saline (PBS) containing 2% heat-inactivated fetal bovine serum (FBS). The bone marrow cells were then subjected to gradient centrifugation at 500 *g* for 5 min, followed by red blood cell lysis using a lysis buffer (provided by BOSTER, Wuhan, China). The cells were suspended in 15% L929 conditional medium (RPMI-1640 medium containing 10% FBS, 1% penicillin/streptomycin, and 15% L929 cell culture supernatant) and incubated at 37°C with 5% CO_2 for 24 h to allow the cells to adhere to the culture dish. The adherent cells were then replated in 6-well plates with 15% L929 conditional medium at a density of 1×10^6 cells per well, and cultured for 7 consecutive days with the medium changed every 2 days to obtain BMDMs. Subsequently, the BMDMs were exposed to a high glucose environment for 48 h: (1) control group (5.5 mM glucose); (2) HG group (35 mM glucose)[22].

For lymphocyte extraction, the kidney tissue was isolated from diabetic nephropathy model mice and placed on a 200 mesh steel screen to grind from the edge, transferring it to a 15 mL centrifuge tube. The tube was centrifuged at 650 rpm for 1 min, and the supernatant was collected into another 15 mL centrifuge tube. After centrifugation at 1,500 rpm for 5 min, the supernatant was discarded and the washing process was repeated twice. The pellet was resuspended in 6 mL of a 40% Percoll solution, and 3 mL of a 70% Percoll solution was added to the bottom layer. The tube was then centrifuged at 2,000 rpm for 20 min, with acceleration and deceleration rates of 6 and 2, respectively. The leukocyte layer between the two layers of Percoll solution was extracted into a 15 mL centrifuge tube, and after the addition of PBS to fill the tube, centrifugation was performed at 200 rpm for 5 min to collect the cells. After resuspending the cells in 1 mL of PBS, 10 μL of the cell suspension was taken and mixed with trypan blue in a 1:1 ratio for cell counting purposes.

Cell transfection

When the cell fusion reached 80–90%, transfection was conducted following the instructions for Lipofectamine 2000 (11668-019, Invitrogen, New York, CA, USA). All plasmids were provided and constructed by the Shanghai Genome Company. Transfection in the HG group was divided into several groups: sh-NC group (negative control silenced plasmid), sh-IGHG1 group (IGHG1 silenced plasmid), sh-TRIM11 group (TRIM11 silenced plasmid), sh-TonEBP group (TonEBP silenced plasmid), DMSO group (solvent control group),

PD98059 group (MEK/ERK inhibitor, 10 μM), sh-TRIM11 + oe-NC group (TRIM11 silenced plasmid + negative control overexpressed plasmid), sh-TRIM11 + oe-ERK group (TRIM11 silenced plasmid + overexpressed ERK plasmid).

Construction of lentiviral vectors for silencing IGHG1, TRIM11, and TonEBP

The pGreenPuro-CMV-shRNA-Lentivector (sh- silencing vector, catalog number: SI505A-1, System Biosciences, USA) was purchased to construct lentivirus-based silencing vectors for IGHG1, TRIM11, and TonEBP. The silencing sequences are listed in Table S1. The lentiviral vectors were transfected into HK-2 cells using Opti-MEM medium (31985070, Gibco) and Lipofectamine 3000 reagent (L3000015, Invitrogen, New York, California, USA, https://www.thermofisher.cn/cn). After 20 h, the growth medium was replaced with 12 mL of medium supplemented with 5% fetal bovine serum. After 48 h of transfection, the supernatant containing the virus was collected, filtered through a 0.45 μm cellulose acetate filter (HAWG04700, MF-Millipore, https://www.sigmaaldrich.cn/), and stored at −80°C.

Establishment of DN mouse models

A total of 40 male C57BL/6 mice at the age of 6–8 weeks were housed in a specific pathogen-free (SPF) animal facility. The laboratory maintained a humidity of 60–65% and a temperature of 22–25°C, with a 12 h light/dark cycle. Free access to food and water was provided. After 7 days of adaptation feeding, routine measurements including blood glucose, blood pressure, blood lipids, and body weight, were taken to confirm the absence of any abnormalities in the mice. The mice were then randomly divided into two groups: a control group consisting of 10 mice and a diabetic nephropathy (DN) group consisting of 110 mice. The control group received an intraperitoneal injection of citrate buffer (0.1 M, pH 4.5). The DN group was fed a high-fat diet (67% basal feed, 10% lard, 20% sugar, 2.5% cholesterol, and 0.5% sodium cholate) for 2 weeks before being intraperitoneally injected with streptozotocin (STZ) at a dose of 50 mg/kg[23]. The mice were then returned to standard laboratory housing. After 3 days of STZ injection, blood samples were collected from the tail or neck vein to measure blood glucose levels. A fasting blood glucose (FBG) level ≥5.6 mmol/L or a blood glucose level ≥78 mmol/L 2 h post-load indicated the preliminary establishment of the model.

After successful model establishment, some DN mice were randomly divided into five groups (n = 10). The groups consisted of the DN group (diabetic nephropathy model), DN + sh-NC group (DN mice injected with 10 μL sh-NC lentivirus *via* the tail vein), DN + sh-IGHG1 group (DN mice injected with 10 μL sh-IGHG1 lentivirus *via* the tail vein), DN + sh-TRIM11 group (DN mice injected with 10 μL sh-TRIM11 lentivirus *via* the tail vein), and DN + sh-TonEBP group (DN mice injected with 10 μL sh-TonEBP lentivirus *via* the tail vein).

Another portion was randomly divided into three groups (n = 10): DN + DMSO group (DN mice injected with 10 μL DMSO *via* the tail vein) and DN + epalrestat group (DN mice injected with 10 μL epalrestat *via* the tail vein).

Yet another portion was randomly divided into three groups (n = 10): DN + sh-NC + oe-NC group (DN mice injected with 10 μL sh-NC lentivirus and oe-NC lentivirus *via* the tail vein), DN + sh-IGHG1 + oe-NC group (DN mice injected with 10 μL sh-IGHG1 lentivirus and oe-NC lentivirus *via* the tail vein), and DNA + sh-IGHG1 + oe-TonEBP group (DN mice injected with 10 μL sh-IGHG1 lentivirus and 10 μL oe-TonEBP lentivirus *via* the tail vein).

After 6 weeks, euthanasia was performed by intraperitoneal administration of 50 mg/kg pentobarbital sodium to all mice. Urine was collected for 24 h before euthanasia for albumin detection. All animal experiments were conducted according to the approved protocol of our institution's Animal Care and Use Committee. The optimal MOI for 10 μL lentivirus was determined to be 50.

ELISA

Serum creatinine (SCr) was measured using the mouse creatinine assay kit (C011-2-1), blood urea nitrogen (BUN) using a urea detection kit (C013-2-1), and albumin using the urine albumin ELISA kit (AO28-2-1)[24]. These kits were from Jian-Cheng Bioengineering Institute (Nanjing, China).

Detection of albumin/creatinine ratio (ACR)

Twenty-four-hour urine samples were collected from each group of mice and analyzed using a urine microalbumin detection kit to measure ACR levels.

H&E staining

Sections were dewaxed, hydrated, stained with hematoxylin (60°C) for 60 s, and hydrolyzed with 1% hydrochloric ethanol for 3 s. After washing for 2 s with 1 × PBS, sections were stained with eosin, dehydrated, and sealed, followed by observation of the morphological structure of the kidney under a microscope[25].

Cellular immunofluorescence double staining method

Cultured macrophages and lymphocytes were seeded onto glass slides for staining. After treatment, the cells were washed trice with PBS and fixed with 4% formaldehyde for 30 min at room temperature. Subsequently, the cells were treated with 0.1% Triton X-100 for 30 min, followed by blocking with 3% normal donkey serum (containing 0.1% Triton X-100) for 1 h in the dark. The cells were then incubated overnight at 4°C with the following primary antibodies: mouse anti-TRIM11 antibody (ab111694, 1:500, Abcam, Cambridge, UK), TonEBP antibody (ab3446, 1:20, Abcam), IGHG antibody (PA5-75428, 1:500, Thermo Fisher, Waltham, MA, USA), macrophage-specific marker F4/80 antibody (ab6640, 1:200, Abcam), or lymphocyte-specific marker CD4 antibody (CD4 Antibody (36-0041-85), 1:200, Invitrogen). Following this, the cells were incubated with two secondary antibodies, Goat Anti-Rat IgG H&L (Alexa Fluor® 488) (1:500, ab150165) and Alexa Fluor555-conjugated

antibody (AB150078, 1:500, Abcam), at 37°C for 1 h. After washing three times with PBS for 5 min each, the cell nuclei were stained with DAPI for 5 min. Subsequently, fluorescence images were captured using an Olympus FLUOVIEW FV1000 confocal laser scanning microscope (Olympus Corporation, Tokyo, Japan). The localization and expression of IGHG1, TRIM11, and TonEBP in DN macrophages and lymphocytes were observed using this microscope (scale: 50 μm; 400× magnification).

Tissue section immunofluorescence double staining method

Frozen kidney tissue sections (5 μm thickness) were obtained, followed by three washes with phosphate-buffered saline (PBS) at room temperature for 5 min each. The slides were then blocked with 5% bovine serum albumin (BSA) for 30 min. Subsequently, they were incubated overnight at 4°C with the following primary antibodies: TRIM11 (ab111694, 1:500, Abcam), TonEBP (ab3446, 1:20, Abcam), IGHG (PA5-75428, 1:500, Thermo Fisher), Wilms tumor-specific marker antibody (Novus Immunologicals, Littleton, NBP2-44607, 1:200), or aquaporin 1 antibody (NB600-749, 1:200). After incubation, the slides were incubated at 37°C for 1 h with secondary antibodies, which included TRITC-labeled antibody (AB6786, 1:500, Abcam) and Alexa Fluor 488-labeled antibody (AB150077, 1:500, Abcam). Subsequently, the slides were washed three times with PBS for 5 min each. Finally, the nuclei were stained with DAPI for 5 min, and the stained sections were imaged using an Olympus FLUOVIEW FV1000 confocal laser scanning microscope (Olympus Corporation, Tokyo, Japan).

RNA extraction and qRT-PCR

The total cellular RNA was extracted strictly as per the manuals of a TRIZOL kit (15596-018, Solarbio, Beijing, China), followed by concentration estimation. cDNA was synthesized using the RNA RT kit (KR116, TianGen Biotechnology Co., Ltd, Beijing, China). The cDNA concentration was determined using fluorescence quantitative PCR (B21202, Bimake, Shanghai, China), and the cDNA was diluted to the same concentration using the quantitative dilution method. The cDNA (1 μL) was acquired, and the reaction amplification system was 10 μL. The reaction was conducted using a fluorescence quantitative PCR instrument Applied Biosystems ViiA™ 7 (Applied Biosystems). The $2^{-\Delta\Delta CT}$ method was applied for fold change calculation normalized to β-actin. Primers were synthesized by Sangon (Shanghai, China) and designed using the Primer5 software (Table S2).

Western blot

Total tissue and cell proteins were extracted, separated, and transferred to membranes. The membrane was blocked with 5% skim milk powder and probed with primary antibodies to TRIM11 (ab111694, 1:1,000, Abcam), TonEBP (ab3446, 1:1,000, Abcam), IGHG1 (PA5-75428, 1:500, Thermo Fisher), ERK1 (ab32537, 1:1,000, Abcam), ERK2 (ab32081, 1:1,000, Abcam), MEK1/2 (#4694, 1:1,000, CST, USA), p-ERK1/2 (ab201015, 1:1,000, Abcam), p-MEK1/2 (#2338, 1:1,000, CST, Danvers, MA) at 4°C overnight. After that, the membrane was re-probed with HRP-labeled secondary IgG antibody (Abcam; goat anti-rabbit: ab205718, 1:20,000 or goat anti-rat: ab6789, 1:5,000). After development, the solution was added for developing, and quantitative analysis of proteins was performed using ImageJ software, normalized to β-actin (ab8226, 1:1,000, Abcam).

Statistical analysis

Data were processed using SPSS 21.0 software, Chicago, IL, USA, with measurement data summarized as mean ± SD. Comparisons between the two groups were analyzed using unpaired *t*-tests and comparisons among multiple groups using one-way ANOVA with Tukey's test. A value of $P < 0.05$ reflects statistical significance.

RESULTS

IGHG1, TRIM11, and TonEBP were predicted bioinformatically to be highly expressed in DN

To explore the mechanisms related to diabetic nephropathy, we conducted differential analysis on the DN-related microarray GSE86300, displaying 12 significantly upregulated and 17 significantly downregulated mRNAs in renal cortex samples of diabetes mellitus mice (Figure 1a,b). By reviewing the literature, we found that among these 12 significantly upregulated genes, only IGHG1 has not been reported in diabetic nephropathy but is remarkably upregulated in chronic kidney disease[15], consistent with the microarray analysis results. Furthermore, we observed upregulation of IGHG1 expression in late-stage diabetic nephropathy by analyzing the GSE20636 and GSE185616 datasets (Figure 1c, d). Immunofluorescence staining revealed elevated expression of IGHG1, TRIM11, and TonEBP in the renal tissue of DN mice, with TonEBP showing predominant enrichment in the renal tubular epithelial cells (Figure 1e). Furthermore, IGHG1, TRIM11, and TonEBP also demonstrated overall high expression in bone marrow-derived macrophages and lymphocytes in diabetic nephropathy (Figure 1f, g). These findings suggest their potential involvement in the inflammatory-driven pathology of diabetic nephropathy.

IGHG1 positively regulated TRIM11 and TonEBP expression *in vitro*

To explore the relationship among IGHG1, TRIM11, and TonEBP, HK-2 cells were treated with HG. IGHG1, TRIM11, and TonEBP were notably higher in HG-treated HK-2 cells than in control cells, as reflected by qRT-PCR and Western blot results (Figure 2a, b). After further silencing IGHG1, IGHG1, TRIM11, and TonEBP, the expression was lowered in HG-treated HK-2 cells with sh-IGHG1 (Figure 2c, d). Silencing of either TRIM11 or TonEBP in HK2 cells of the HG group did not yield significant changes in the expression of IGHG1 (Figure 2e–h). However, compared with the sh-NC group, the silencing of TRIM11 and TonEBP resulted in a notable reduction in their expression levels (Figure 2e, f). In summary, IGHG1 positively orchestrated TRIM11 and TonEBP expression *in vitro*.

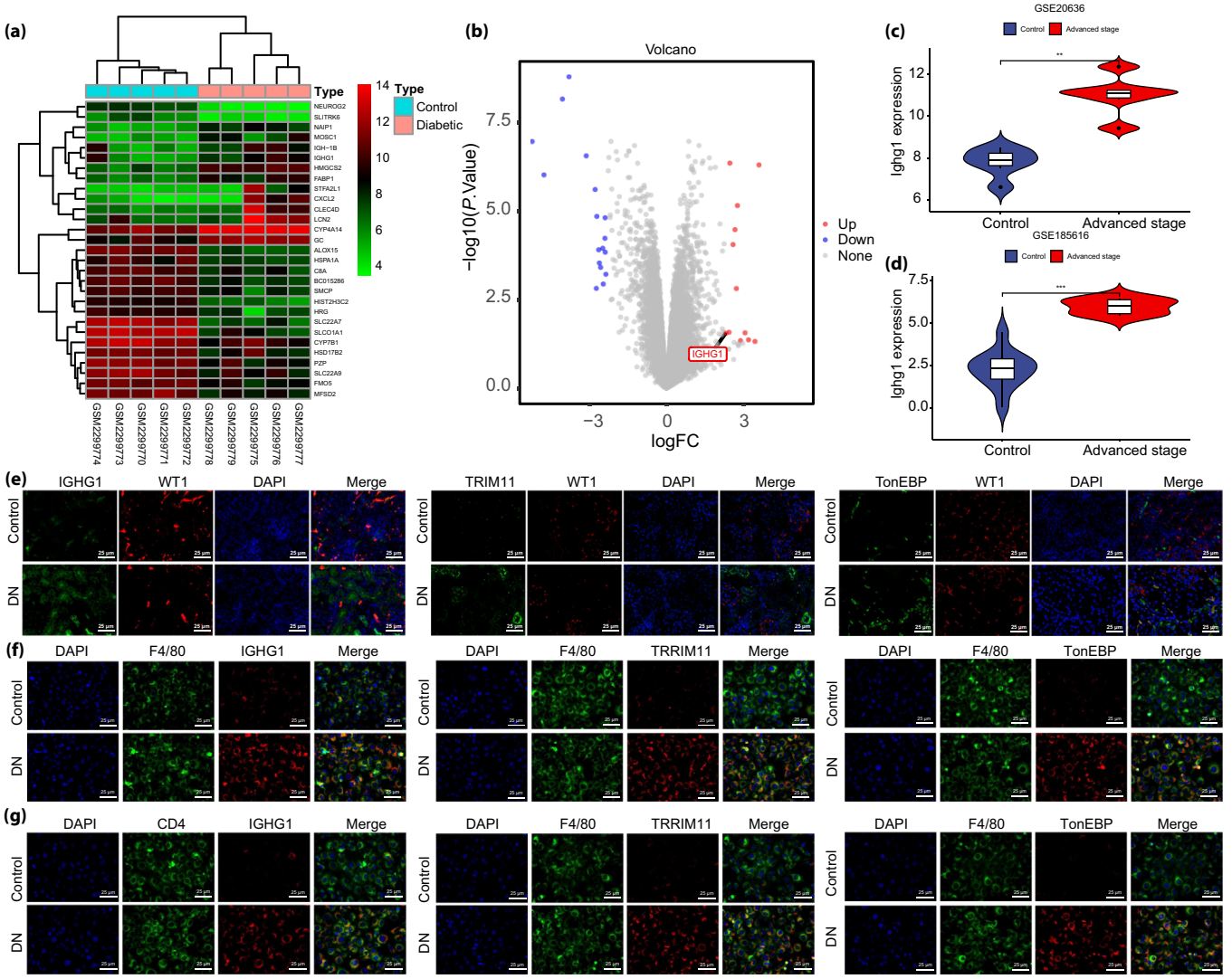

Figure 1 | Bioinformatics screening of key genes correlated with diabetic nephropathy. (a) Heatmap depicting the expression of significantly differentially expressed mRNAs in the renal cortex samples of early diabetic mice from the GSE86300 dataset. (b) Volcano plot illustrating the significantly differentially expressed mRNAs in the renal cortex samples of early diabetic mice from the GSE86300 dataset, with red indicating upregulation and blue indicating downregulation. (c) Expression levels of IGHG1 in the renal tissue samples of late diabetic mice and control samples from the GSE20636 dataset, $P < 0.001$, $P < 0.005$. (d) Expression levels of IGHG1 in the renal cortex samples of late diabetic mice and control samples from the GSE185616 dataset. (e) Cellular localization of IGHG1, TRIM11, and TonEBP in diabetic kidneys. Immunofluorescence double staining was performed on mouse kidney tissues from the control and DN groups using antibodies against p-μ/IGHG1, p-μ/TRIM11, p-μ/TonEBP, and the renal tubular epithelial cell marker WT1 (scale bar = 100 μm; 400× magnification). IGHG1, TRIM11, and TonEBP (green), WT1 (red), and DAPI (blue). (f, g) Immunofluorescence staining was used to detect the expression of IGHG1 (red), TRIM11 (red), and TonEBP (red) in DN macrophages (marked with F4/80, green) and lymphocytes (marked with CD4, green) (scale bar: 50 μm; 400× magnification). Control = 5, DN = 5. *$P < 0.05$ when compared with the control group.

TRIM11 upregulated TonEBP expression through the activation of the MEK/ERK pathway *in vitro*

The study further dissected the mechanism of TRIM11 and TonEBP in diabetic nephropathy. qRT-PCR and Western blot results exhibited successful TRIM11 transfection (Figure 3a). The Western blot results demonstrated (Figure 3b) that compared with the sh-NC group, the sh-TRIM11 group exhibited a significant decrease in the ratios of p-MEK1/2 to MEK1/2, p-ERK1/2 to ERK1/2, as well as a reduction in TonEBP expression levels.

Further, qRT-PCR and Western blot data (Figure 3c) indicated that PD98059 diminished TonEBP expression in HG-treated HK-2 cells. Further, TRIM11 and the MEK/ERK pathway were altered to verify that TRIM11 mediated TonEBP

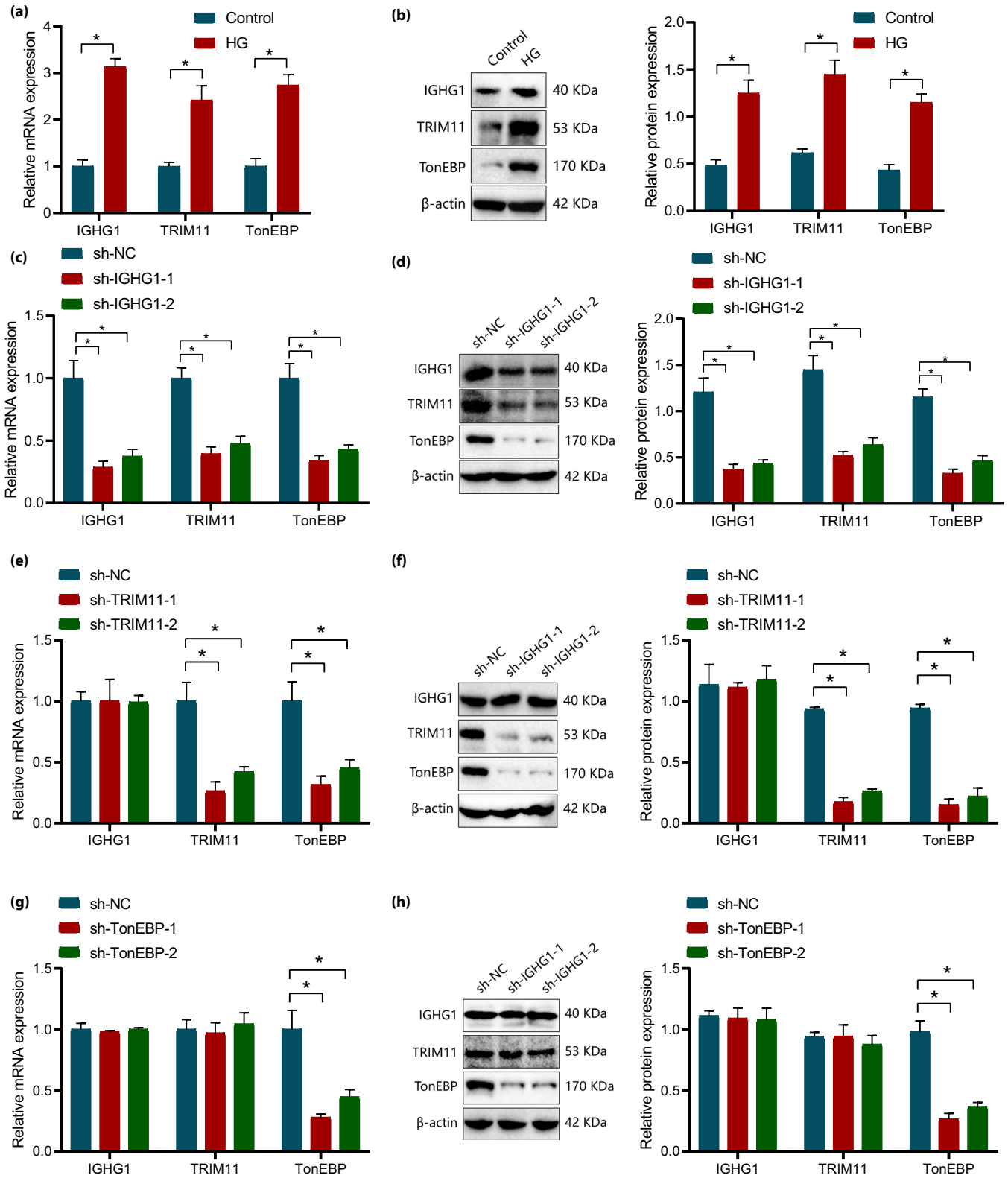
(a)
Control
HG
Relative mRNA expression
IGHG1
TRIM11
TonEBP
(b)
Control
HG
IGHG1
TRIM11
TonEBP
β-actin
40 KDa
53 KDa
170 KDa
42 KDa
Relative protein expression
(c)
sh-NC
sh-IGHG1-1
sh-IGHG1-2
(d)
sh-NC
sh-IGHG1-1
sh-IGHG1-2
(e)
sh-NC
sh-TRIM11-1
sh-TRIM11-2
(f)
sh-NC
sh-TRIM11-1
sh-TRIM11-2
(g)
sh-NC
sh-TonEBP-1
sh-TonEBP-2
(h)
sh-NC
sh-TonEBP-1
sh-TonEBP-2

Figure 2 | IGHG1 silencing decreases TRIM11 and TonEBP expression in HG-induced HK-2 cells. (a, b) IGHG1, TRIM11, and TonEBP expression in HG-induced HK-2 cells was measured by qRT-PCR (a) and Western blot (b). (c, d) IGHG1, TRIM11, and TonEBP expression in HG-induced HK-2 cells after silencing IGHG1 measured by qRT-PCR (c) and Western blot (d). (e, f) The expression levels of IGHG1, TRIM11, and TonEBP in the cells from each group were evaluated using qRT-PCR and Western blot analysis after TRIM11 knockdown. (g, h) The expression levels of IGHG1, TRIM11, and TonEBP in the cells from each group were evaluated using qRT-PCR and Western blot analysis after TonEBP knockdown. *$P < 0.05$ compared with the control or sh-NC groups. An independent samples *t*-test was employed to compare between two groups, while a one-way analysis of variance (ANOVA) was used for multiple group comparisons. Cell experiments were repeated three times.

through the MEK/ERK pathway. For qRT-PCR results (Figure 3d), unchanged TRIM11 expression and increased ERK and TonEBP expression were observed following treatment with oe-ERK + sh-TRIM11. Western blot results (Figure 3e) also manifested unchanged TRIM11 expression and elevated p-ERK1/2, ERK, and TonEBP expression upon treatment with oe-ERK + sh-TRIM11. Collectively, TRIM11 enhanced TonEBP expression *via* MEK/ERK pathway activation *in vitro*.

Silencing of IGHG1 alleviated symptoms of DN in mice

Further, we established a mouse model of diabetic nephropathy for validation. In the DN group, the kidney weight/body weight ratio increased but decreased after silencing IGHG1, TRIM11, and TonEBP (Figure 4a). The ELISA results (Figure 4b–e) showed that compared with the control group, the DN group exhibited a significant increase in blood creatinine and blood urea nitrogen expression, increased urinary albumin, and a notable increase in ACR levels. Treatment with sh-IGHG1, sh-TRIM11, and sh-TonEBP could reverse the above results. Compared with the DN + DMSO group, the DN + epalrestat group showed a decrease in kidney weight/body weight ratio in mice(Figure S1A) and significantly decreased blood creatinine and blood urea nitrogen expression, urinary albumin, and ACR levels (Figure S1A–E). The H&E staining results (Figure 4f) revealed that compared with the control group, the DN group exhibited disrupted renal tubular epithelium, renal tubular vascular clusters, and interstitial structures, enlarged renal glomeruli, widened mesangial areas, noticeable matrix proliferation, thickened glomerular basement membrane, and tubular atrophy and dilation, as well as vacuolar degeneration of tubular epithelial cells, formation of tubular casts, and minimal infiltration of inflammatory cells in the tubulointerstitium. Silencing IGHG1 alleviated the renal damage, resulting in milder lesions. Compared with the

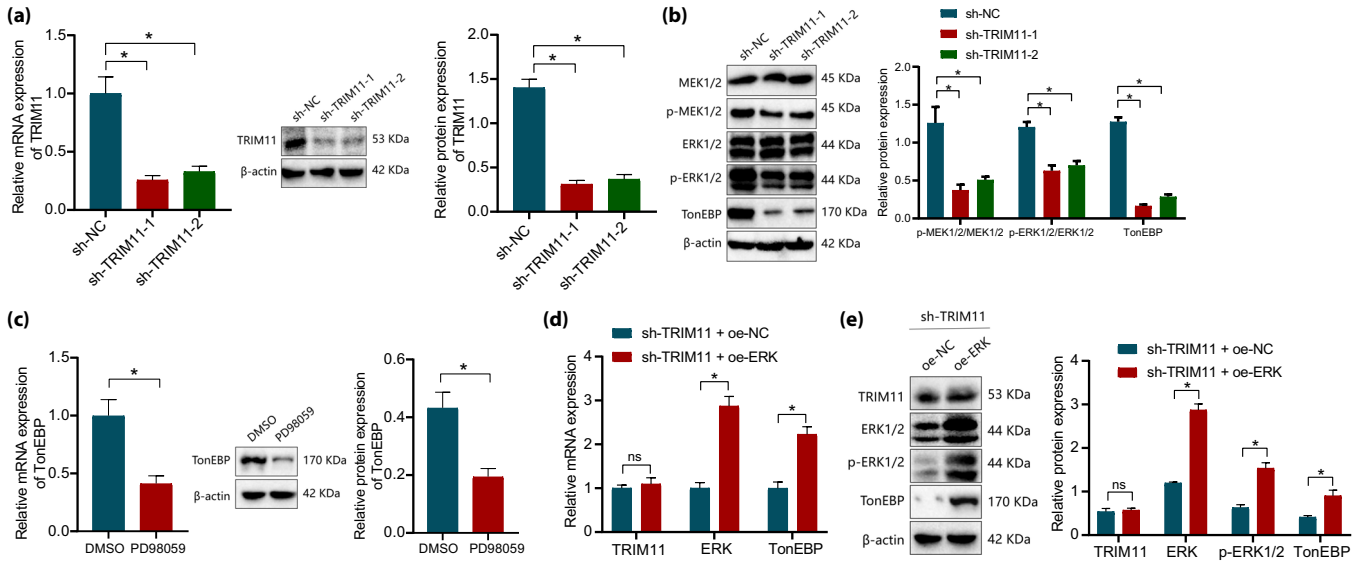

Figure 3 | TRIM11 silencing blocks the MEK/ERK pathway to downregulate TonEBP expression in HG-treated HK-2 cells. (a) The transfection efficiency of TRIM11 detected by qRT-PCR and Western blot (*$P < 0.05$, **$P < 0.01$ compared with the sh-NC group). (b) Western blot determined the expression of p-MEK1/2, p-ERK1/2, and TonEBP (*$P < 0.05$, P compared with the sh-NC group). (c) The expression of TonEBP measured by qRT-PCR and Western blot (*$P < 0.05$ compared with the DMSO group). (d) qRT-PCR detection of ERK and TonEBP expression. (e) Western blot analysis of the expression of ERK, p-ERK1/2, and TonEBP (ns indicates no statistical difference compared with the sh-TRIM11 + oe-NC group, *$p < 0.05$ compared with the sh-TRIM11 + oe-NC group). An independent samples *t*-test was employed to compare between two groups, while ANOVA was used for multiple group comparisons. Cell experiments were repeated three times.

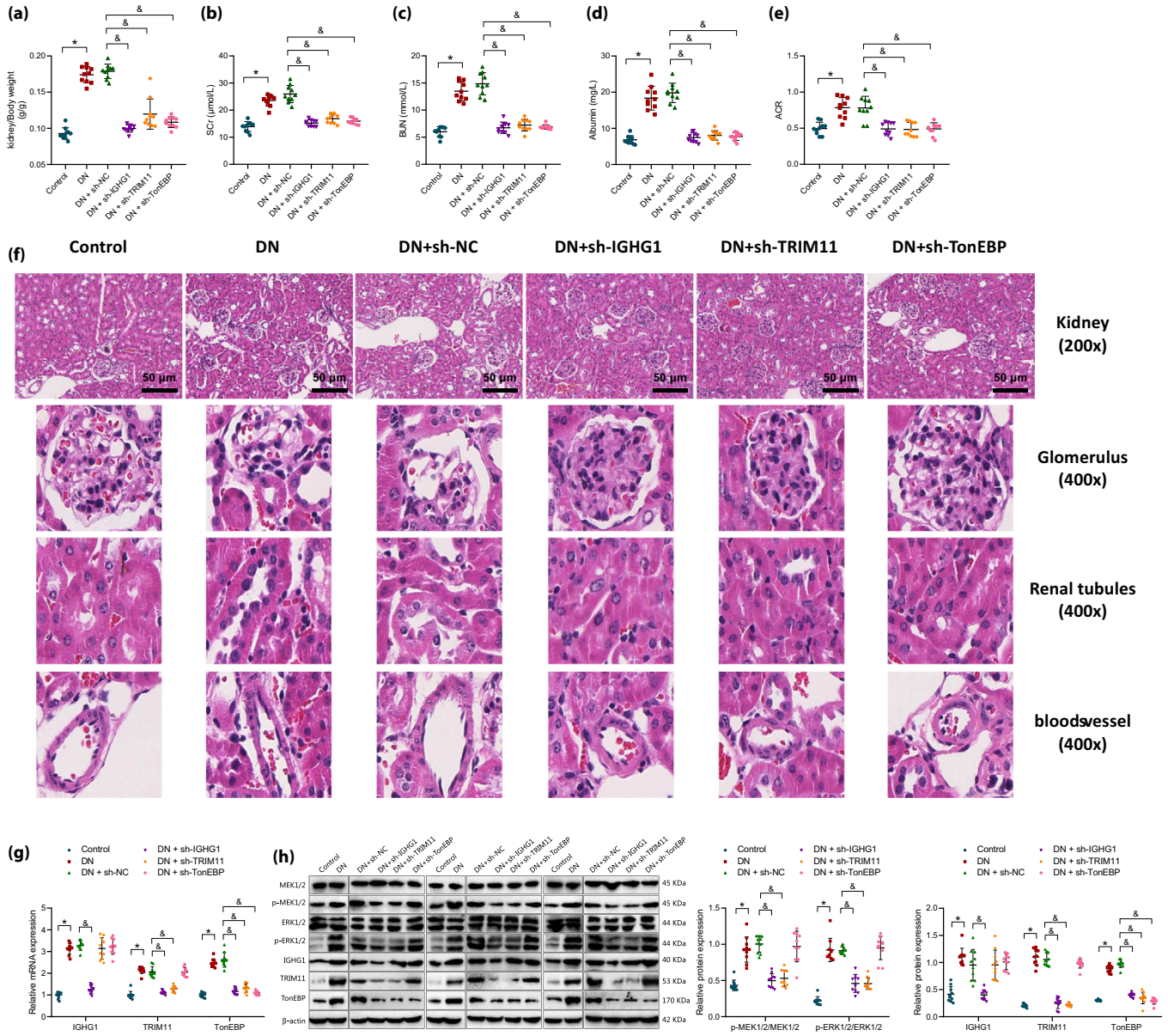

Figure 4 | Silencing of IGHG1 inhibits the progression of diabetic nephropathy in mice. (a) Kidney weight/body weight of mice. (b) ELISA for SCr in mice. (c) ELISA for BUN in mice. (d) ELISA for urinary albumin in mice. (e) Urinary microalbumin detection for ACR levels. (f) H&E staining was used to observe the histopathological damage in the kidney, glomerulus, and blood tissues of the mice in the experimental groups at 200× magnification (scale bar = 50 μm) and 400× magnification (scale bar = 100 μm). (g, h) The expression of relevant genes, including IGHG1, TRIM11, TonEBP, MEK, ERK, p-MEK1/2, and p-ERK1/2 in the renal cortex and medulla of the mice in the experimental groups was evaluated using qRT-PCR and Western blot analysis. *$P < 0.05$ compared with the control group, $^{\&}P < 0.05$ compared with the DN + sh-NC group. ANOVA was used for multiple group comparisons. $n = 10$ for experimental animals in each group.

DN + DMSO group, the DN + epalrestat group showed improvements in DN mouse lesions (Figure S1F).

The qRT-PCR and Western blot results (Figure 4g, h) demonstrated that compared with the control group, IGHG1, TRIM11, and TonEBP expressions were upregulated in the kidney tissues of the DN group, while MEK1/2 and ERK1/2 expressions remained unchanged. The ratio of p-MEK1/2 and p-ERK1/2 to total protein increased significantly. There were no significant differences between the DN and DN + sh-NC groups. Compared with the DN + sh-NC group, the DN + sh-IGHG1 group showed significant downregulation of IGHG1, TRIM11, and TonEBP expressions, while MEK1/2 and ERK1/2

expressions remained unchanged. The ratio of p-MEK1/2 and p-ERK1/2 to total protein decreased. The DN + sh-TRIM group exhibited significant downregulation of TRIM11 and TonEBP expressions, while MEK1/2 and ERK1/2 expressions remained unchanged. The ratio of p-MEK1/2 and p-ERK1/2 to total protein decreased. Conversely, the DN + sh-TonEBP group showed significant downregulation of TonEBP expression, while MEK1/2, ERK1/2, p-MEK1/2, and p-ERK1/2 to total protein expressions remained unchanged. Compared with the DN + DMSO group, the DN + epalrestat group achieved similar results to the DN + sh-IGHG1 group (Figure S1G, H).

These results indicate that silencing IGHG1 can prevent the occurrence and progression of diabetic nephropathy.

Silent expression of IGHG1 and overexpression of TonEBP can induce the occurrence and development of diabetic nephropathy

Additionally, following the silent expression of IGHG1 and overexpression of TonEBP, there was an increase in the kidney weight-to-body weight ratio in mice (Figure 5a). The ELISA results demonstrated that compared with the DN + sh-IGHG1 + oe-NC group, the mice in the DN + sh-IGHG1 + oe-TonEBP group showed a significantly increased expression of blood creatinine and blood urea nitrogen, as well as elevated levels of urinary albumin and ACR (Figure 5b–e). The H&E staining results revealed that compared with the DN + sh-IGHG1 + oe-NC group, the mice in the DN + sh-IGHG1 +

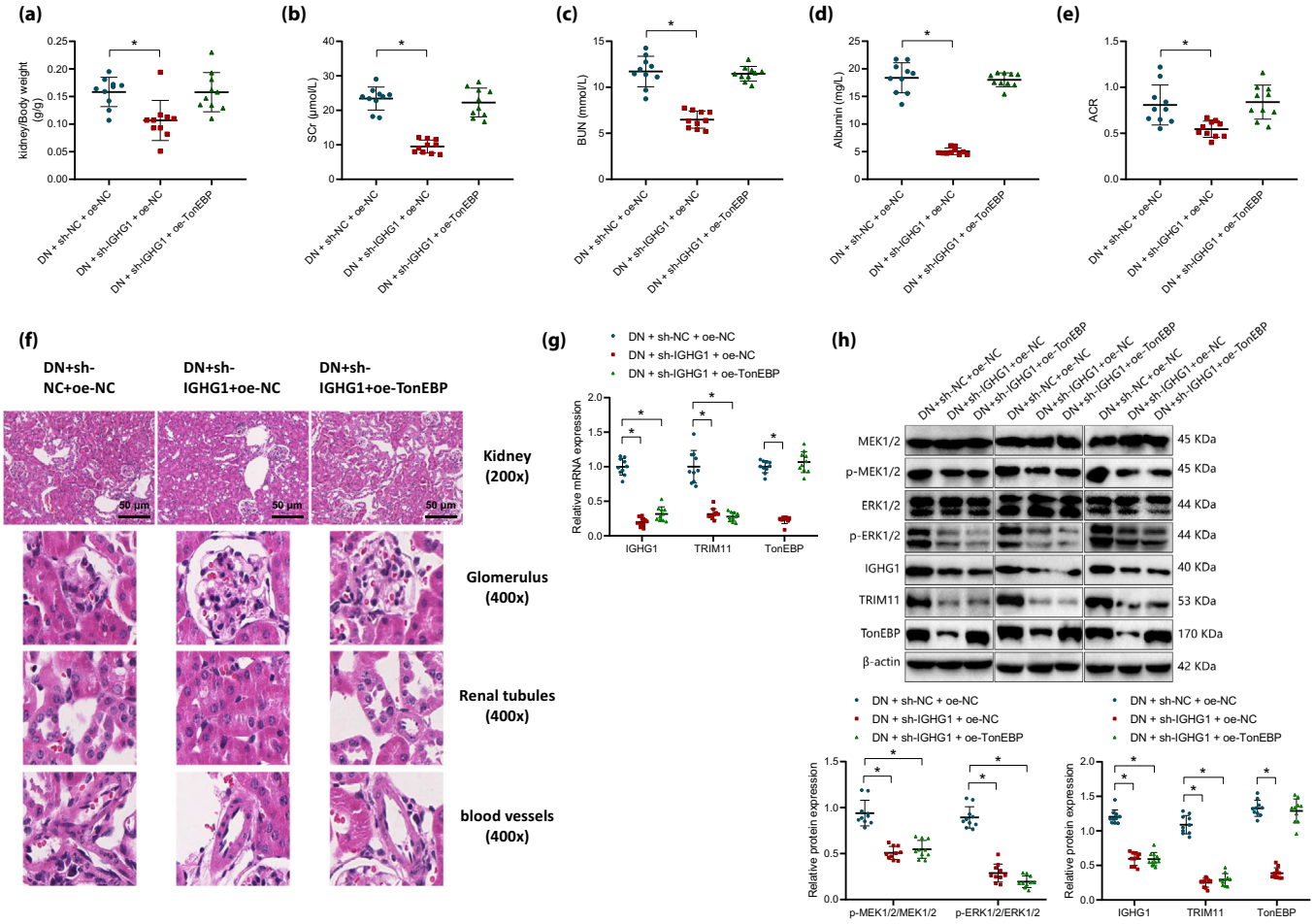

Figure 5 | The effects of silencing IGHG1 and overexpressing TonEBP on the progression of diabetic nephropathy in mice. The following measurements were conducted in this study: (a) renal weight to body weight ratio in each group of mice; (b) serum creatinine levels in each group of mice, measured using ELISA; (c) blood urea nitrogen levels in each group of mice, measured using ELISA; (d) urinary albumin levels in each group of mice, measured using ELISA; (e) urinary microalbumin levels, measured using ACR; (f) pathological damage to kidney, glomerulus, and vascular tissues in the major groups of mice observed through H&E staining (magnification: 200×, scale bar: 50 μm; magnification: 400×, scale bar: 100 μm); (g, h) expression of genes related to IGHG1, TRIM11, TonEBP, MEK, ERK, p-MEK1/2, and p-ERK1/2 was assessed in the renal cortex and medulla of each group of mice using qRT-PCR and Western blot analysis. *$P < 0.05$ compared with the DN + sh-NC + oe-NC group. An independent samples *t*-test was employed to compare two groups, while ANOVA was used for multiple group comparisons. The experiments were replicated three times, with a sample size of $n = 10$ animals per group.

oe-TonEBP group exhibited pathological features similar to DN mice, including disrupted renal tubular epithelium, renal tubule vascular clusters, and interstitial structures, as well as pronounced matrix proliferation and severe lesions (Figure 5f). On the other hand, the DN + sh-IGHG1 + oe-NC group showed reduced renal damage.

Furthermore, qRT-PCR and Western blot results demonstrated that compared with the DN + sh-NC + oe-NC group, the DN + sh-IGHG1 + oe-NC group displayed significant downregulation of IGHG1, TRIM11, and TonEBP expression, while the expression of MEK1/2 and ERK1/2 remained unchanged. The ratio of p-MEK1/2, p-ERK1/2, p-MEK1/2, and p-ERK1/2 to total protein expression decreased. In comparison with the DN + sh-IGHG1 + oe-NC group, the DN + sh-IGHG1 + oe-TonEBP group exhibited decreased expression of IGHG1, TRIM11, MEK1/2, ERK1/2, p-MEK1/2, and p-ERK1/2 in renal tissue, while TonEBP expression was significantly upregulated (Figure 5g, h).

These findings demonstrate that the silent expression of IGHG1 and overexpression of TonEBP can induce the occurrence and progression of diabetic nephropathy.

DISCUSSION

Diabetic nephropathy is a multifactorial disorder with multiple pathogenic molecular processes and histopathological structures[26,27]. Therefore, understanding the molecular mechanism underpinning the progression of diabetic nephropathy is vital for treating this disease better. Based on this, this study was conducted to elucidate the mechanism of IGHG1 in diabetic nephropathy development *via* the TRIM11/MEK/ERK/TonEBP axis. Our data deciphered that silencing IGHG1 prevented the progression of diabetic nephropathy by blocking the TRIM11/MEK/ERK axis and downregulating TonEBP.

As reported, the upregulation of IGHG1, which encodes the heavy chain of IgG, is related to increased immune cell infiltration[28]. Furthermore, elevated immune cell infiltration is critical in the progression of diabetic nephropathy[29]. In addition, prior work observed IgG deposits in the glomeruli of non-obese diabetic mice[30]. Nevertheless, limited studies directly dissect the role of IGHG1 in diabetic nephropathy, despite mounting evidence elucidating the link of IGHG1 upregulation to kidney-related disorders, such as clear cell renal cell carcinoma and chronic kidney disease[15,31]. The molecular assessment of gene transcript patterns, particularly renal compartments, has gained attention in recent years, but knowledge of the mechanisms by which they act still needs to be improved. Prior evidence indicates the involvement of IGHG1 upregulation in the tubulointerstitium with antibody-mediated rejection of renal allografts[32]. Besides, increased IGHG1 was found in B cells of blood samples of active systemic lupus erythematosus[33].

TRIM proteins assume a role in tumor development, proliferation, migration, and apoptosis[34]. In addition, these proteins are also implicated in diabetes mellitus and its complications[35]. For instance, TRIM32 orchestrates insulin resistance by repressing the plakoglobin function in several catabolic states, including diabetes mellitus[36]. In addition, ectopic TRIM13 constrains mesangial collagen synthesis in diabetic nephropathy[37]. Importantly, TRIM11 expression was observed in a previous study to be amplified in the kidney tissues of DN mice[17]. Corroborating results were observed in our work as TRIM11 was upregulated in DN and HG-induced HK-2 cells. Intriguingly, silencing IGHG1 caused the downregulation of TRIM11. Overall, IGHG1 silencing might decrease TRIM11 expression to impede the progression of diabetic nephropathy.

Of note, TRIM11 knock-down curtails cell proliferation and invasion in high-grade glioma by disrupting the MEK/ERK pathway[18]. Furthermore, the activated MEK/ERK pathway by NOD2 contributes to endothelial-to-mesenchymal transition in glomerular vascular endothelial cells to accelerate the development of diabetic nephropathy[38]. Also, blockade of the MEK/ERK pathway is implicated in the repressive impacts of long non-coding RNA ANRIL knock-down on mouse mesangial cell fibrosis, proliferation, and inflammation in diabetic nephropathy[39]. Our data illustrated the decline of p-MEK1/2 and p-ERK1/2 expression in HG-induced HK-2 cells following TRIM11 silencing and in DN mice after IGHG1 silencing. As reported, the MEK/ERK pathway leads to the transactivation of TonEBP in the nucleus pulposus cells of the intervertebral disc[40]. TonEBP (also named Nuclear Factor of Activated T-Cells 5) results in aldose reductase gene upregulation in monocytes, which is linked to early diabetic nephropathy in humans[41]. The haplodeficiency of TonEBP diminishes the activation of macrophages triggered by hyperglycemia, macrophages in the kidney, and the renal expression of pro-inflammatory factors, thus facilitating diabetic nephropathy in mice[42]. In our work, silencing IGHG1 or TRIM11 or inhibiting the MEK/ERK pathway caused a reduction of TonEBP expression *in vitro*. Moreover, TonEBP was downregulated in DN mice by silencing IGHG1.

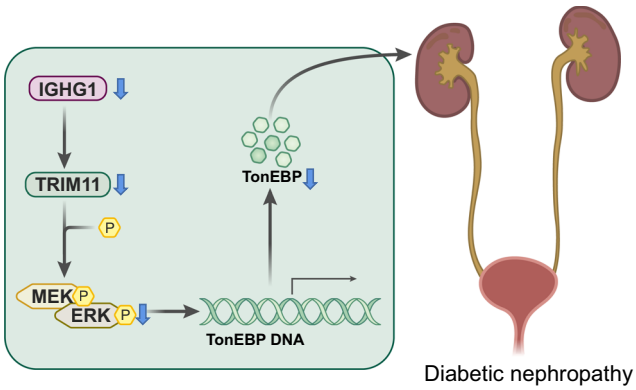

Figure 6 | Molecular mechanism graph of IGHG1 in diabetic nephropathy. IGHG1 elevates TonEBP expression by activating the TRIM11/MEK/ERK pathway, thus alleviating diabetic nephropathy.

In conclusion, our data supported the notion that silencing IGHG1 blocked the TRIM11/MEK/ERK axis to downregulate TonEBP and impeded the progression of diabetic nephropathy (Figure 6). This study first unraveled the relationship between IGHG1 and TRIM11 and disclosed the repression of diabetic nephropathy *via* IGHG1 silencing, which provides potential targets for preventing diabetic nephropathy. Nonetheless, more detailed explorations are merited to dissect further the mechanism of the IGHG1/TRIM11/MEK/ERK/TonEBP axis in diabetic nephropathy.

ACKNOWLEDGMENTS
None declared.

DATA AVAILABILITY STATEMENT
The data supporting this study's findings are available from the corresponding author upon reasonable request.

DISCLOSURE
The authors declare no conflict of interest.
Approval of the research protocol: All animal experiments were conducted by the approved protocol of our institution's Animal Care and Use Committee of the Second Hospital of Jilin University.
Informed consent: N/A.
Registry and the registration no. of the study/trial: N/A.
Animal studies: All animal experiments were conducted by the approved protocol of our institution's Animal Care and Use Committee of the Second Hospital of Jilin University (No. 20210147; Approval date of Registry: 2021.09.13).

REFERENCES
1. Samsu N. Diabetic nephropathy: Challenges in pathogenesis, diagnosis, and treatment. *Biomed Res Int* 2021; 2021: 1497449.
2. Qi C, Mao X, Zhang Z, *et al*. Classification and differential diagnosis of diabetic nephropathy. *J Diabetes Res* 2017; 2017: 8637138.
3. Pavkov ME, Collins AJ, Coresh J, *et al*. Kidney disease in diabetes, 3rd edition. Bethesda (MD): National Institute of Diabetes and Digestive and Kidney Diseases. 2021.
4. Reutens AT, Atkins RC. Epidemiology of diabetic nephropathy. *Contrib Nephrol* 2011; 170: 1–7.
5. Umanath K, Lewis JB. Update on diabetic nephropathy: Core curriculum 2018. *Am J Kidney Dis* 2018; 71: 884–895.
6. Zoja C, Xinaris C, Macconi D. Diabetic nephropathy: Novel molecular mechanisms and therapeutic targets. *Front Pharmacol* 2020; 11: 586892.
7. Li X, Chen W, Yang C, *et al*. IGHG1 upregulation promoted gastric cancer malignancy via AKT/GSK-3beta/beta-Catenin pathway. *Cancer Cell Int* 2021; 21: 397.
8. Zhang J, Zhang J, Zhang R, *et al*. Implications of immunoglobulin G deposit in glomeruli in Chinese patients with diabetic nephropathy. *J Diabetes* 2020; 12: 521–531.
9. Abdou AE, Anani HAA, Ibrahim HF, *et al*. Urinary IgG, serum CX3CL1 and miRNA-152-3p: as predictors of nephropathy in Egyptian type 2 diabetic patients. *Tissue Barriers* 2022; 10: 1994823.
10. Li X, Ni R, Chen J, *et al*. The presence of IGHG1 in human pancreatic carcinomas is associated with immune evasion mechanisms. *Pancreas* 2011; 40: 753–761.
11. Zhang M, Li Z, Li J, *et al*. Revisiting the pig IGHC gene locus in different breeds uncovers nine distinct IGHG genes. *J Immunol* 2020; 205: 2137–2145.
12. Bashirova AA, Zheng W, Akdag M, *et al*. Population-specific diversity of the immunoglobulin constant heavy G chain (IGHG) genes. *Genes Immun* 2021; 22: 327–334.
13. Vivekanandan-Giri A, Slocum JL, Buller CL, *et al*. Urine glycoprotein profile reveals novel markers for chronic kidney disease. *Int J Proteomics* 2011; 2011: 214715.
14. Kalantari S, Nafar M, Rutishauser D, *et al*. Predictive urinary biomarkers for steroid-resistant and steroid-sensitive focal segmental glomerulosclerosis using high resolution mass spectrometry and multivariate statistical analysis. *BMC Nephrol* 2014; 15: 141.
15. Zhou Q, Xiong Y, Huang XR, *et al*. Identification of genes associated with Smad3-dependent renal injury by RNA-seq-based transcriptome analysis. *Sci Rep* 2015; 5: 17901.
16. Sauter MM, Brandt CR. Knockdown of TRIM5alpha or TRIM11 increases lentiviral vector transduction efficiency of human Muller cells. *Exp Eye Res* 2021; 204: 108436.
17. Chen W, Peng R, Sun Y, *et al*. The topological key lncRNA H2k2 from the ceRNA network promotes mesangial cell proliferation in diabetic nephropathy via the miR-449a/b/Trim11/Mek signaling pathway. *FASEB J* 2019; 33: 11492–11506.
18. Di K, Linskey ME, Bota DA. TRIM11 is overexpressed in high-grade gliomas and promotes proliferation, invasion, migration and glial tumor growth. *Oncogene* 2013; 32: 5038–5047.
19. Huang X, Tan J, Li Y, *et al*. Expression of LncRNA KCNQ1Ot1 in diabetic nephropathy and its correlation with MEK/ERK signaling pathway. *Am J Transl Res* 2022; 14: 1796–1806.
20. Kojima R, Taniguchi H, Tsuzuki A, *et al*. Hypertonicity-induced expression of monocyte chemoattractant protein-1 through a novel cis-acting element and MAPK signaling pathways. *J Immunol* 2010; 184: 5253–5262.
21. Hashimoto Y, Yamagishi S, Mizukami H, *et al*. Polyol pathway and diabetic nephropathy revisited: Early tubular cell changes and glomerulopathy in diabetic mice overexpressing human aldose reductase. *J Diabetes Investig* 2011; 2: 111–122.
22. Liu J, Zhang Y, Sheng H, *et al*. Hyperoside suppresses renal inflammation by regulating macrophage polarization in mice with type 2 diabetes mellitus. *Front Immunol* 2021; 12: 733808.
23. Liu XQ, Jiang L, Li YY, *et al*. Wogonin protects glomerular podocytes by targeting Bcl-2-mediated autophagy and

apoptosis in diabetic kidney disease. *Acta Pharmacol Sin* 2022; 43: 96–110.
24. Yan JJ, Lee JG, Jang JY, *et al*. IL-2/anti-IL-2 complexes ameliorate lupus nephritis by expansion of $CD4^+CD25^+Foxp3^+$ regulatory T cells. *Kidney Int* 2017; 91: 603–615.
25. Luo D, Dai W, Feng X, *et al*. Suppression of lncRNA NLRP3 inhibits NLRP3-triggered inflammatory responses in early acute lung injury. *Cell Death Dis* 2021; 12: 898.
26. Sagoo MK, Gnudi L. Protocols. Diabetic nephropathy: an overview. *Methods Mol Biol* 2020; 2067: 3–7.
27. Tziomalos K, Athyros VG. Diabetic nephropathy: New risk factors and improvements in diagnosis. *Rev Diabet Stud* 2015; 12: 110–118.
28. Wang G, Li H, Pan J, *et al*. Upregulated expression of cancer-derived immunoglobulin G is associated with progression in glioma. *Front Oncol* 2021; 11: 758856.
29. Yu K, Li D, Xu F, *et al*. IDO1 as a new immune biomarker for diabetic nephropathy and its correlation with immune cell infiltration. *Int Immunopharmacol* 2021; 94: 107446.
30. Xiao X, Ma B, Dong B, *et al*. Cellular and humoral immune responses in the early stages of diabetic nephropathy in NOD mice. *J Autoimmun* 2009; 32: 85–93.
31. Chen Y, Liang Y, Chen Y, *et al*. Identification of prognostic metabolism-related genes in clear cell renal cell carcinoma. *J Oncol* 2021; 2021: 2042114.
32. Trailin A, Mrazova P, Hruba P, *et al*. Chronic active antibody-mediated rejection is associated with the upregulation of interstitial but not glomerular transcripts. *Front Immunol* 2021; 12: 729558.
33. Blanco IK, Heuer S, Catalina M, *et al*. Tissue infiltration of plasma cells/plasmablasts in patients with active systemic lupus erthematosus (SLE). *J Immunol* 2017; 198: 55.8.
34. Shang M, Weng L, Xu G, *et al*. TRIM11 suppresses ferritinophagy and gemcitabine sensitivity through UBE2N/TAX1BP1 signaling in pancreatic ductal adenocarcinoma. *J Cell Physiol* 2021; 236: 6868–6883.
35. Wan T, Li X, Li Y. The role of TRIM family proteins in autophagy, pyroptosis, and diabetes mellitus. *Cell Biol Int* 2021; 45: 913–926.
36. Cohen S, Lee D, Zhai B, *et al*. Trim32 reduces PI3K-Akt-FoxO signaling in muscle atrophy by promoting plakoglobin-PI3K dissociation. *J Cell Biol* 2014; 204: 747–758.
37. Li Y, Ren D, Shen Y, *et al*. Altered DNA methylation of TRIM13 in diabetic nephropathy suppresses mesangial collagen synthesis by promoting ubiquitination of CHOP. *EBioMedicine* 2020; 51: 102582.
38. Shang J, Zhang Y, Jiang Y, *et al*. NOD2 promotes endothelial-to-mesenchymal transition of glomerular endothelial cells via MEK/ERK signaling pathway in diabetic nephropathy. *Biochem Biophys Res Commun* 2017; 484: 435–441.
39. Fang X, Hu J, Zhou H. Knock-down of long non-coding RNA ANRIL suppresses mouse mesangial cell proliferation, fibrosis, inflammation via regulating Wnt/beta-Catenin and MEK/ERK pathways in diabetic nephropathy. *Exp Clin Endocrinol Diabetes* 2022; 130: 30–36.
40. Tsai TT, Guttapalli A, Agrawal A, *et al*. MEK/ERK signaling controls osmoregulation of nucleus pulposus cells of the intervertebral disc by transactivation of TonEBP/OREBP. *J Bone Miner Res* 2007; 22: 965–974.
41. Yang B, Hodgkinson AD, Oates PJ, *et al*. Elevated activity of transcription factor nuclear factor of activated T-cells 5 (NFAT5) and diabetic nephropathy. *Diabetes* 2006; 55: 1450–1455.
42. Choi SY, Lim SW, Salimi S, *et al*. Tonicity-responsive enhancer-binding protein mediates hyperglycemia-induced inflammation and vascular and renal injury. *J Am Soc Nephrol* 2018; 29: 492–504.

SUPPORTING INFORMATION

Additional supporting information may be found online in the Supporting Information section at the end of the article.

Figure S1 | The impact of EPALRESTAT silencing on the progression of diabetic nephropathy in mice.

Table S1 | shRNA sequence information

Table S2 | Primers used for qRT-PCR